ISSN 1096-6080 (PRINT) ISSN 1096-0929 (ONLINE)

Volume 153 | Number 1 | September 2016

Toxicological Sciences

THE OFFICIAL JOURNAL OF THE SOCIETY OF TOXICOLOGY

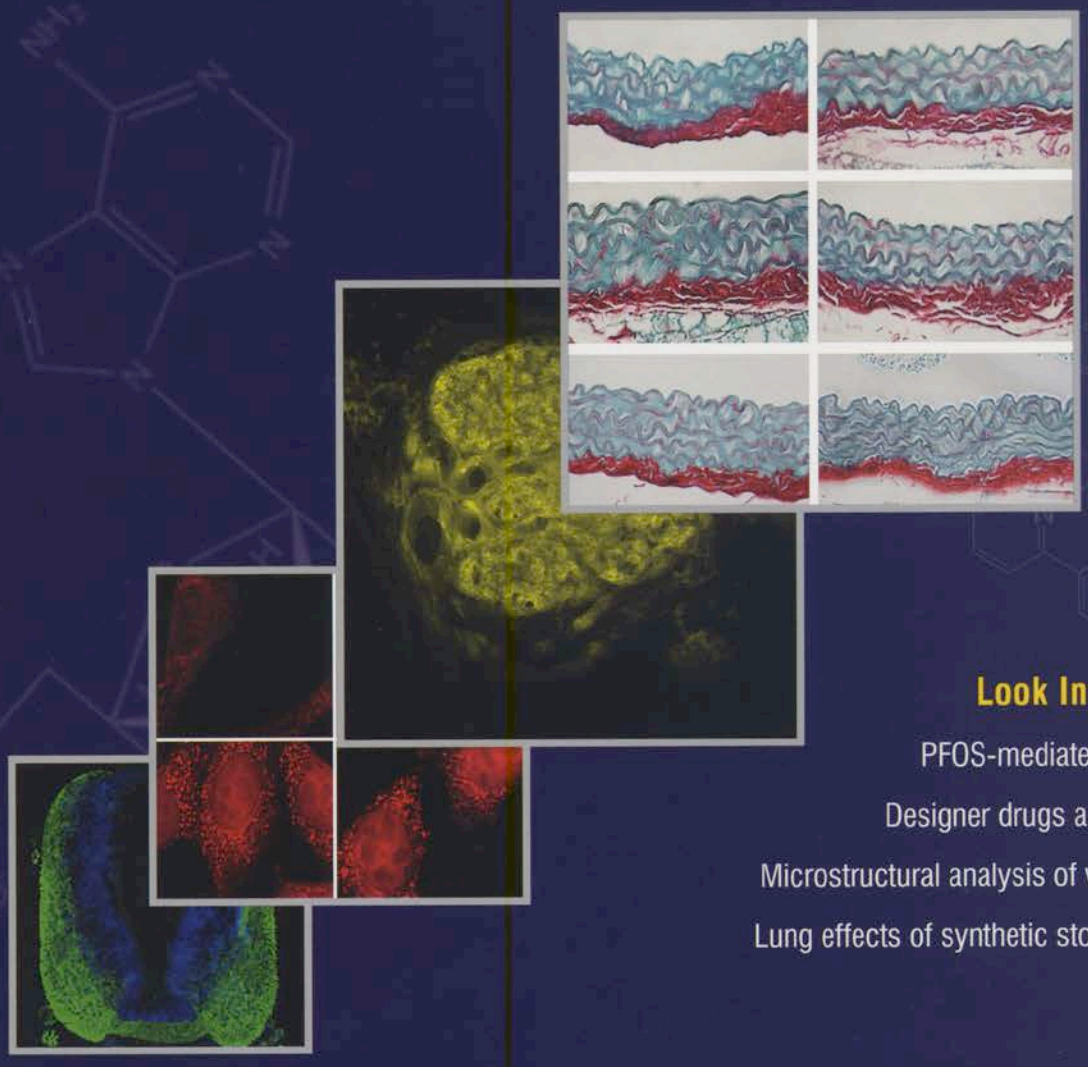

Look Inside ToxSci

PFOS-mediated liver damage

Designer drugs and liver toxicity

Microstructural analysis of welders' brains

Lung effects of synthetic stone particulates

OXFORD UNIVERSITY PRESS

SOT | Society of Toxicology

www.toxsci.oxfordjournals.org

OXFORD
SOT | Society of Toxicology
www.toxsci.oxfordjournals.org

TOXICOLOGICAL SCIENCES, 153(1), 2016, 1

doi: 10.1093/toxsci/kfw136
Look Inside ToxSci

look inside ToxSci

From the Editor's Desk

In this month's editorial, I opine on the state of scientific literature and the importance of high-quality publications. It reminds me of the value of journals like *Toxicological Sciences*. With the backing of the Society of Toxicology, *Toxicological Sciences* seeks to add value to the scientific enterprise. Papers published in the journal undergo an extensive level of peer review to assure that the scientific quality meets our high standards. In this issue, we have informative papers on the toxicological effects of occupational and recreational exposures, ranging from artificial stones, to manganese, to designer drugs. I encourage you to look inside *ToxSci* for the best original research (and literature) in the field of toxicology.—Gary W. Miller

Editor's Highlights

Designer drugs and liver toxicity: Cathinone designer drugs (derivatives of β-keto amphetamines) have been increasingly used for recreational purposes, but the assessment of their adverse effects has been limited. One of the more notable adverse effects of these drugs, colloquially referred to as bath salts, is significant liver damage. The paper by Valente *et al.* (pp. 89-102) examines common indicators of cellular stress and toxicity using primary rat hepatocytes and HepaRG cells. The authors observed that each of the 4 drugs tested (hydrochloride salts of methylone, 3,4-methylenedioxypyrovalerone, pentedrone, and 4-methylethcathinone) were capable of eliciting reactive oxygen and nitrogen species, and depleting glutathione. The 2 most toxic compounds, 3,4-methylenedioxypyrovalerone and pentedrone, were also capable of depleting ATP levels. The study identifies oxidative stress and mitochondrial dysfunction as key mechanisms in the apoptotic cell death of hepatic cells that may contribute to liver damage in users of these drugs. View Abstract—Nathan Cherrington

Occupational exposure to man-made stone products: The report by Pavan *et al.* (pp. 4-17) addresses the concern that processing of man-made artificial stone, a composite of quartz, metals, and agglomerated pigments and resins, is promoting occupational pulmonary fibrosis. The work carefully analyzes particle composition and characterizes the potential for cytotoxicity, cell membrane lysis, and epithelial-to-mesenchymal cell transition in relevant cell types compared to the well-characterized effects of the reference quartz material Min-U-Sil 5. The authors showed that the resin content of the dusts can reduce the membrane lysing and cytotoxic effects of the particles; however, the resin is lost in biologically relevant thermal degradation, revealing the underlying toxicity of the quartz/metal composites. The high metal content of the particles produces excess oxidant generation and promotes epithelial-to-mesenchymal transition, a hallmark and potential underlying mechanism of fibrosis. This study provides evidence that exposure to highly reactive particles of respirable size can increase risk of fibrosis, which may inform regulations for the safe production of products from the artificial stone. As indicated in the title, advanced man-made materials may generate ancient dust-related disease that has been an occupational health concern for millennia. View Abstract—Aaron Barchowsky

Microstructural changes in brains of welders exposed to manganese: Welding causes occupational exposure to manganese (Mn) and to other metals such as iron and copper. This has been associated with a variety of neurobehavioral disorders including Mn-induced parkinsonism, which shares several features of Parkinson's disease. The study by Lee *et al.* in this issue of *ToxSci* (pp. 165-173) adds new information on the array of tools available to assess preclinical changes in the brain of Mn-exposed workers. Using magnetic resonance imaging, they identified a specific change in "fractional anisotropy" (reflective of microstructural alterations) in an area of the brain of welders known as the globus pallidus. The globus pallidus is a known target of Mn and is also affected in Parkinson's disease. Interestingly, these changes were only seen upon long-term exposure (>20 years) to Mn and appear related to exposure to Mn itself and not to other metals. As workers presenting such morphological changes did not present any behavioral symptoms, this approach may help identify early changes in brain structure and function in asymptomatic workers. View Abstract—Lucio G. Costa

Role of choline in PFOS-mediated liver toxicity: Perfluorooctane sulfonate (PFOS) has been shown to cause hepatic steatosis and reduce total serum cholesterol levels, but the mechanism underlying these effects is not known. In the article by Zhang *et al.* (pp 186-197) the investigators tested the hypothesis that PFOS forms an ion pair with choline. Mice were fed either choline-deficient or choline-supplemented diets to determine the effects of altered choline on PFOS-mediated steatosis and cholesterol homeostasis. Previous studies have shown that severe restriction of dietary choline can cause steatosis. Reduced dietary choline exacerbated the effects of PFOS, while increased dietary choline mitigated the adverse effects of choline. The authors conducted an extensive analysis of PFOS distribution, cholesterol levels, oxidative stress, and hepatic function to support the hypothesis that PFOS binds to choline, thereby reducing available choline needed for cholesterol biosynthesis and export. View Abstract—Gary W. Miller

OXFORD

SOT | Society of Toxicology
www.toxsci.oxfordjournals.org

TOXICOLOGICAL SCIENCES, 153(1), 2016, 186–197

doi: 10.1093/toxsci/kfw120
Advance Access Publication Date: July 13, 2016
Research Article

Perfluorooctane Sulfonate-Choline Ion Pair Formation: A Potential Mechanism Modulating Hepatic Steatosis and Oxidative Stress in Mice

Limin Zhang,*,[1] Prasad Krishnan,*,[1] David J. Ehresman,† Philip B. Smith,‡ Mainak Dutta* Bradford D. Bagley,† Shu-Ching Chang,† John L. Butenhoff,§ Andrew D. Patterson,* and Jeffrey M. Peters*,[2]

*Department of Veterinary and Biomedical Science and Center for Molecular Toxicology and Carcinogenesis, The Pennsylvania State University, University Park, Pennsylvania 16802; †Medical Department, 3M Company, St Paul, Minnesota; ‡The Huck Institutes of the Life Sciences, The Pennsylvania State University, University Park, Pennsylvania; and §SaluTox, L.L.C, Lake Elmo, Minnesota

[1]These authors contributed equally to this study.
[2]To whom correspondence should be addressed at Department of Veterinary and Biomedical Science and Center for Molecular Toxicology and Carcinogenesis, The Pennsylvania State University, University Park, PA 16802. Fax: 814-863-1696. E-mail: jmp21@psu.edu.

ABSTRACT

The mechanisms underlying perfluorooctane sulfonate (PFOS)-induced steatosis remain unclear. The hypothesis that PFOS causes steatosis and other hepatic effects by forming an ion pair with choline was examined. C57BL/6 mice were fed either a control diet or a marginal methionine/choline-deficient (mMCD) diet, with and without 0.003, 0.006, or 0.012% potassium PFOS. Dietary PFOS caused a dose-dependent decrease in body weight, and increases in the relative liver weight, hepatic triglyceride concentration and serum markers of liver toxicity and oxidative stress. Some of these effects were exacerbated in mice fed the mMCD diet supplemented with 0.012% PFOS compared with those fed the control diet supplemented with 0.012% PFOS. Surprisingly, serum PFOS concentrations were higher while liver PFOS concentrations were lower in mMCD-fed mice compared with corresponding control-fed mice. To determine if supplemental dietary choline could prevent PFOS-induced hepatic effects, C57BL/6 mice were fed a control diet, or a choline supplemental diet (1.2%) with or without 0.003% PFOS. Lipidomic analysis demonstrated that PFOS caused alterations in hepatic lipid metabolism in the PFOS-fed mice compared with controls, and supplemental dietary choline prevented these PFOS-induced changes. Interestingly, dietary choline supplementation also prevented PFOS-induced oxidative damage. These studies are the first to suggest that PFOS may cause hepatic steatosis and oxidative stress by effectively reducing the choline required for hepatic VLDL production and export by forming an ion pair with choline, and suggest that choline supplementation may prevent and/or treat PFOS-induced hepatic steatosis and oxidative stress.

Key words: perfluorooctane sulfonate; liver; choline; steatosis; mechanism.

Perfluorooctane sulfonate ($C_8F_{17}SO_3^-$, PFOS) is an exceptionally stable, highly electronegative fluorosurfactant resistant to environmental and metabolic degradation. The principal use of PFOS is in extreme environments such as aqueous film forming foam in firefighting and acid mist suppression in electroplating. PFOS may also arise from the degradation of its manufacturing precursors, perfluorooctane sulfonyl fluoride ($C_8F_{18}SO_2$, POSF), or perfluorooctane sulfonamide-based compounds (Xu *et al.* 2004). PFOS has been detected in human serum at concentrations in the ng/ml range in the general population (Hansen *et al.*

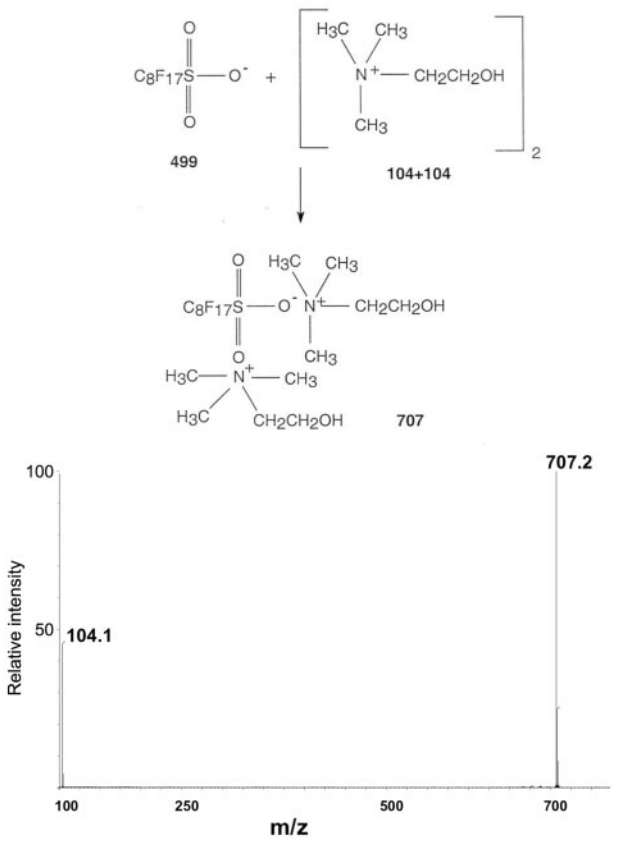

FIG. 1. PFOS/choline ion pair formation. PFOS and choline were incubated and analyzed by infusing the solution into a Waters G2S quadrupole time-of-flight mass spectrometer operating in ESI+. Tandem MS of the putative PFOS/choline pair identified 104+ corresponding to choline. PFOS is not detectable in ESI+ mode and therefore is not present in the mass spectra.

2001), with an estimated serum elimination half-life of approximately 5 years (Olsen *et al.* 2007). These findings have increased interest in potential human health risk from exposure to PFOS.

Based on studies in cynomolgus monkeys, the earliest effect of repeated PFOS dosing is a decrease in serum total cholesterol (Seacat *et al.*, 2002). This decrease is likely due to impairment of hepatic lipoprotein production, based on mechanistic studies in the APOE*3-Leiden.CETP mouse model (Bijland *et al.*, 2011). In rodents, PFOS can activate the peroxisome proliferator-activated receptor-α (PPARα), which is known to increase hepatic lipid catabolism and contribute to hypolipidemia (Akiyama *et al.*, 2001). Interestingly, hepatic steatosis was observed after exposure to PFOS in cynomolgus monkeys and APOE*3-Leiden.CETP mice (Bijland *et al.*, 2011; Seacat *et al.*, 2002). In considering the decreased production of VLDL and the observed hepatic steatosis in these models, it is of interest to note that non-alcoholic hepatic steatosis and reduced serum lipids can be produced by feeding a methionine and choline deficient diet (MCD) in mice (Marcolin *et al.*, 2011). Moreover, steatosis and reductions in serum lipids caused by feeding an MCD diet in experimental animal models resemble those observed after dosing with PFOS. Prior unpublished work from our group has confirmed that a molecule of PFOS can form stable ion-pairs with 2 molecules of choline in phosphate-buffered saline when observed over a period of up to 6 days using liquid chromatography-mass spectrometry/mass spectrometry (LC-MS/MS) analyses (Figure 1). Thus, it is plausible that PFOS also forms ion-pairs with choline in animals, which subsequently results in insufficient choline supply leading to steatosis. Although this ion pair was not detected in liver from PFOS-treated mice, or from naïve rat liver spiked with PFOS *in vitro*, such detection may be hampered by the energies required for the LC-MS/MS analysis.

In this study, the hypothesis that an hepatic in situ ion-pair forms between PFOS and choline *in vivo* after oral exposure to PFOS and contributes to the mechanism for the PFOS-induced hepatic steatosis was examined. This hypothesis was tested by examining whether feeding a marginal MCD diet (mMCD) would exacerbate the hepatic steatotic effects of dietary PFOS, and mitigated by feeding a diet supplemented with choline.

MATERIALS AND METHODS

Animals. Male C57BL/6 mice, 8- to 10-weeks old, were used for all the experiments reported herein. Mice were housed in an Association for Assessment and Accreditation of Laboratory Animal Care accredited facility, with a temperature (25°C) and light (12-h light/12-h dark) controlled environment. All animal use protocols were approved by The Pennsylvania State University Institutional Animal Care and Use Committee.

Chemicals. Potassium PFOS (K+PFOS; FC-95, Lot 217, 87% purity) was provided by the 3M Company. Impurities in PFOS have been previously described and consisted primarily of shorter chain homologues of PFOS (Seacat et al., 2002). Chemicals and reagents used in the biochemical and lipidomic studies were of the highest purity available.

Diets. A summary of the diets used for all studies is provided in Table 1. The diets were prepared by Dyets, Inc. (Bethlehem, Pennsylvania). A semi-purified AIN-93G diet was used as the control diet for all studies. An mMCD diet was prepared using a formulation that caused gradual progression of steatosis, based on previous unpublished data. The control and mMCD diets were prepared with identical macro- and micronutrients except the control diet contained 3.0 g L-methionine/kg diet and 4.2 g choline bitartrate/kg diet, whereas the mMCD diet contained 0.009 g L-methionine/kg diet and 0.012 g choline bitartrate/kg diet. The control and mMCD diet were prepared with 0.000, 0.003 (30 mg/kg), 0.006 (60 mg/kg), or 0.012% (120 mg/kg) K^+PFOS (not adjusted for the purity of PFOS). Stock K^+PFOS powder was mixed with sucrose, then added to the diet formulation to achieve target dietary concentrations of K^+PFOS while maintaining a constant level of added sucrose. The dietary content of PFOS was confirmed by LC-MS/MS. The dietary PFOS concentrations were designed to achieve estimated ratios of PFOS to choline ranging from 0, 1, 2, and 4. For the supplemental choline diet study, the control diet (with or without 0.003% K^+PFOS) was prepared with either 4.2 or 12.0 g choline bitartrate/kg diet.

MS/MS of PFOS/choline ion pair. PFOS (10 μM) was incubated at room temperature with 10 μM choline (Sigma) in 60% aqueous acetonitrile modified with 10 mM ammonium acetate. The solution was infused (5 μl/min) into a Waters Synapt G2S quadrupole time-of-flight mass spectrometer operating in electrospray ionization positive mode (ESI+). Product ion tandem mass spectra of the parent ion [M+H] = 707.1+ representing the putative PFOS bound by two choline molecules were obtained following fragmentation using a fixed collision energy (35 V).

mMCD diet study. This study was performed in duplicate and in each replicate, mice were randomly divided into 8 groups

TABLE 1. Composition of Diets Uses for Studies

Study	Base diet	% PFOS	Choline[a] (g/kg diet)
mMCD diet study	Control	—	4.2
mMCD diet study	Control	0.003	4.2
mMCD diet study	Control	0.006	4.2
mMCD diet study	Control	0.012	4.2
mMCD diet study	mMCD	—	0.012
mMCD diet study	mMCD	0.003	0.012
mMCD diet study	mMCD	0.006	0.012
mMCD diet study	mMCD	0.012	0.012
Study	**Base diet**	**% PFOS**	**Choline[a] (g/kg diet)**
PFOS uptake study	Control	—	4.2
PFOS uptake study	Control	0.012	4.2
PFOS uptake study	mMCD	—	0.012
PFOS uptake study	mMCD	0.012	0.012
Study	**Diet**	**% PFOS**	**Choline[a] (g/kg diet)**
Choline supp. study	Control	—	4.2
Choline supp. study	Control	0.003	4.2
Choline supp. study	Control + choline	—	12.0
Choline supp. study	Control + choline	0.003	12.0

[a]Choline bitartrate.

(5–6 mice/group), and fed the control diet for 2 weeks. After this acclimation period, groups of mice were fed one of the following experimental diets: control diet with or without 0.003, 0.006, or 0.012% K^+PFOS, or the mMCD diet with or without 0.003, 0.006, or 0.012% K^+PFOS (Table 1), for either 23 days (first replicate) or 21 days (second replicate). Because 2 mice in the first replicate fed the mMCD diet with 0.012% K^+PFOS became moribund and were euthanized between 21 and 23 days of treatment, the first replicate was terminated after 23 days and the second replicate was limited to 21 days of feeding. Accordingly, the final group size was 5 mice/group in the first replicate except for the mMCD + 0.012% K^+PFOS group, which was 4. For the second replicate, the experiment was repeated as described earlier with all groups having 5 mice/group, except for the group fed the mMCD diet with 0.012% K^+PFOS, where 6 mice were used, one of which became moribund and was euthanized just prior to scheduled termination of treatment, leaving a final group size of 5.

In each experimental replicate, mice were euthanized after termination of the experimental dietary treatment. Blood was obtained from each mouse and serum fractions were isolated and frozen (−80°C) until further analyses. Livers were carefully dissected, weighed and either fixed in 10% phosphate buffered formalin (PBF) or snap frozen in liquid nitrogen and stored at −80°C until further analyses as described below. Average body weight and relative liver weight per group were calculated. From the first replicate, serum was analyzed for markers of liver toxicity (alanine aminotransferase (ALT), bile acids, and total bilirubin), and both serum and liver concentration of PFOS as previously described. (Chang *et al.*, 2012) From the second replicate, serum and liver samples were used for metabolomic analysis (data not shown). Histopathological analyses were performed on liver samples from both experimental replicates.

PFOS uptake/excretion analyses. Mice were randomly divided into four groups (5 mice/group) and fed the control diet for 2 weeks. After this acclimation period, groups of mice were fed either the control diet (with or without 0.012% K^+PFOS), or the mMCD diet (with or without 0.012% K^+PFOS) (Table 1). After 1 week of dietary treatment, mice were placed in metabolic cages for urine and feces collection. After 24 h, urine and fecal samples were weighed/measured and body weights were recorded. Mice were then euthanized followed by blood (processed to serum) and liver collection (weight recorded). All the samples collected (urine, feces, serum, and liver) were snap frozen in liquid nitrogen and stored at −80°C before PFOS analyses as previously described (Chang *et al.*, 2012).

Choline supplementation study. Mice were randomly divided into four groups (5 mice/group) and fed the control diet for 2 weeks. After this acclimation period, mice were fed one of the following diets for 6 weeks: the control diet (with or without 0.003% K^+PFOS), or the control supplemental choline diet (with or without 0.003% K^+PFOS; Table 1). Body weights were recorded weekly. The mice were euthanized after 6 weeks of feeding the experimental diets, and blood (processed to serum) and liver were collected. Liver samples were weighed, and a small section was fixed in PBF for histological analyses. Liver and serum samples were snap frozen in liquid nitrogen and stored at −80°C pending PFOS analyses as previously described in Chang *et al.* (2012).

Histopathology. Liver sections were fixed in 10% PBF for 48 h, transferred to 70% ethanol, and embedded with paraffin followed by 5 μm sectioning using a microtome. The thin sections were stained with hematoxylin and eosin (H&E), and examined with a light microscope and observations were noted by a board certified pathologist.

Serum markers of liver function. The VetScan Mammalian Liver Profile reagent rotors were used with the VetScan Chemistry Analyzer (Abaxis, Inc., Union City, California) to quantify serum markers of liver function: ALT activity, bile acids, and total bilirubin.

Oil red O and osmium tetroxide staining. Fresh liver samples were embedded in optimal cutting temperature compound, frozen, and cryosectioned. Frozen sections were stained with Oil Red O (ORO) or osmium tetroxide for qualitative examination and morphologic evaluation. The stained histologic sections were examined by light microscopy and observations were noted by a board certified pathologist. Histologic sections were of adequate size and quality for detailed evaluation, and the number of tissues examined from each treatment group was sufficient to allow detection of test article-related histologic alterations.

Liver slides stained with ORO were scanned at 20× magnification using the Hamamatsu NanoZoomer whole slide scanner (Hamamatsu Corp., Middlesex, New Jersey) and virtual slides were imported into the Visiopharm software platform (Visopharm, Broomfield, Colarado). An image analysis protocol was created to identify the ORO positive tissue and 40% of the tissue section was sampled by systematic uniform random sampling at 20× magnification. The percentage of ORO positive area within the liver section was calculated automatically by the software for each animal (represented in the data tables as the percent area of lipid). White areas and artifacts such as folds, tears, and large air bubbles were excluded from the analysis.

Liver slides stained with osmium tetroxide were scanned at 20× magnification as described earlier. An image analysis protocol was created to identify the osmium positive tissue and

100% of the tissue section was sampled by systematic uniform random sampling at 20× magnification. The percentage of osmium positive area within the liver section was calculated automatically by the software for each animal (represented in the data tables as the percent area of lipid). White areas and artifacts such as folds, tears, and large air bubbles were excluded from the analysis.

Lipidomics. Lipids were extracted from flash frozen liver samples using the Folch extraction method (Folch *et al.*, 1957). Briefly, liver samples (~50 mg) were homogenized using a PreCellys Tissue Homogenizer (Bertin Technologies, Rockville, Maryland) for 30 s at 6500 rpm in 1 ml 2:1 chloroform/methanol solution with zirconium beads. The samples were then allowed to incubate at room temperature for five minutes, vortexed briefly, and centrifuged at 4°C for 20 min at maximum speed and the lower organic phase transferred to a new microcentrifuge tube. Two hundred microliters of HPLC grade water was added to the separated organic phase, vortexed for 30 s, and centrifuged at 2000 rpm. for 5 min and the lower organic phase transferred to a new microcentrifuge tube. The samples were then dried under a gentle stream of nitrogen (Savant speedvac, ThermoScientific, Waltham, Massachusetts) and reconstituted in 0.1% formic acid, 10 mM ammonium formate, and 300 µl of a solution containing isopropanol:acetonitrile:water (45:35:20 v/v/v).

Samples (5 µl) were separated by reverse phase HPLC using a Prominence 20 UFLCXR system (Shimadzu, Columbia, Maryland) with a Waters (Milford, Massachusetts) CSH C18 column (100 × 2.1 mm 1.7 µm particle size) maintained at 55°C and a 20-min aqueous/acetonitrile/isopropanol gradient, at a flow rate of 225 µl/min. Solvent A was 40%water, 60% acetonitrile with 10 mM ammonium formate and 0.1% formic acid, and solvent B was 90% isopropanol 10% acetonitrile 10 mM ammonium formate, and 0.1% formic acid. The initial conditions were 60% solvent A and 40% solvent B, increasing to 43% solvent B at 2 min, 50% solvent B at 2.1 min, 54% solvent B at 12 min, 70% solvents B at 12.1 min, and 99% solvent B at 18 min, held at 99% solvent B until 20 min before returning to the initial conditions. The eluate was delivered into a 5600 TripleTOF using a Duospray ion source (SCIEX, Framingham, Massachusetts). The capillary voltage was set at 5.5 kV in positive ion mode and 4.0 kV in negative ion mode with a declustering potential of 80 V used in both modes. The mass spectrometer was operated in Information Dependent Acquisition mode with a 100 ms survey scan from 100 to 1200 m/z, and up to 20 MS/MS product ion scans (100 ms) per duty cycle using collision energy of 50 V with a 20 V spread.

Mass spectrometry data preprocessing, lipid annotation. After data acquisition, the spectral files were imported in MarkerView software (SCIEX, Framingham, Massachusetts) for data preprocessing. The positive and negative mode spectra were separately aligned using the following parameters: minimum spectral peak width, 3 ppm; minimum retention time peak width, 4 scans; RT tolerance, 0.80 min and mass tolerance, 25–30 ppm. The aligned spectra were normalized to total intensity. Lipid annotation was performed based on precursor ion search using METLIN. An additional MS/MS search was performed by matching experimental with predicted spectral fragmentation using LipidBlast (Kind *et al.*, 2013). LipidMaps was also used for verification when applicable (Fahy *et al.*, 2007). All mass spectral identifications were manually verified based on class characteristic fragmentation patterns involving their head groups and fatty acyl side chains. A chemical similarity score matrix was generated using PubChem. Cytoscape edge attributes were then built using MetaMapp. Finally the lipid network was plotted in Cytoscape (Shannon *et al.*, 2003).

Malondialdehyde assay. The malondialdehyde (MDA) assay kit was purchased from Cayman Chemicals (Ann Arbor, Michigan) and hepatic MDA was quantified according to manufacturer's recommended procedures.

Glutathione and oxidized glutathione measurements. Hepatic Glutathione (GSH) and oxidized glutathione (GSSG) were quantified as described previously in Lu *et al.* (2010).

Statistical analysis. Statistical analyses were performed using one-way ANOVA followed by Bonferroni's *post-hoc* analyses (Prism 5.0d, GraphPad Software Inc., La Jolla, California). Average values were considered statistically significant when $P \leq .05$ using *post-hoc* analyses.

RESULTS

Marginal Methionine/Choline Deficiency Exacerbates PFOS-Induced Hepatic Effects

For this study, for the control diets supplemented with K^+PFOS targeted at 0.003, 0.006, and 0.012%, respectively, the measured PFOS concentrations were (average ± SD): 0.0026% ± 0.0004, 0.0052% ± 0.0008, and 0.0127% ± 0.0006. For the marginal methionine/choline deficiency (mMCD) diets supplemented with K^+PFOS targeted at 0.003, 0.006, and 0.012%, respectively, the measured PFOS concentrations were 0.0022% ± 0.0001, 0.0044% ± 0.0004, and 0.0117% ± 0.0007.

When compared with mice fed the control diet, K^+PFOS caused a dose-dependent decrease in body weights, and the reduction was statistically significant in mice fed with 0.012% K^+PFOS at the end of week 2 and onward (Figure 2A). Mice fed the mMCD diet alone also exhibited weight loss as compared with control mice at the end of week 2 and onward (Figure 2A). Weight loss was more severe in mice fed the mMCD diet with 0.012% K^+PFOS as compared with all other groups at the end of week 2 and onward (Figure 2A).

Relative liver weight was increased by dietary K^+PFOS and this effect was similar between mice fed the control or the mMCD diet (Figure 2B). Dietary PFOS administration caused an increase in serum ALT, bile acids and bilirubin fed the control diet (Figure 2C). Serum ALT, bile acids and bilirubin were also generally higher in the mice fed the mMCD diet as compared with those fed the control diet (Figure 2C). However, these increases were markedly higher in the mice fed the mMCD diet with 0.012% K^+PFOS as compared with mice fed the control diet with 0.012% K^+PFOS (Figure 2C).

Histological evaluation of fixed liver tissue revealed ground-glass cytoplasmic alterations that were present in hepatocytes of mice from all groups that received PFOS, independent of concentration or diet (control or mMCD; Figure 2D). The severity of the ground-glass cytoplasmic alteration was generally dose-associated in PFOS-treated groups. Macrovesicular hepatocellular vacuolation was present in mice fed the control diet with 0.006 or 0.012% K^+PFOS, but not in mice fed the control diet or control diet with 0.003% K^+PFOS (Figure 2D). In contrast, mice fed the mMCD diet with or without PFOS had a high incidence of macrovesicular vacuolation. It is of interest to note that the degree of macrovesicular vacuolation in mice fed the mMCD diet with 0.012% K^+PFOS was less pronounced than that in mice fed the mMCD diet with 0.0, 0.003, or 0.006% K^+PFOS

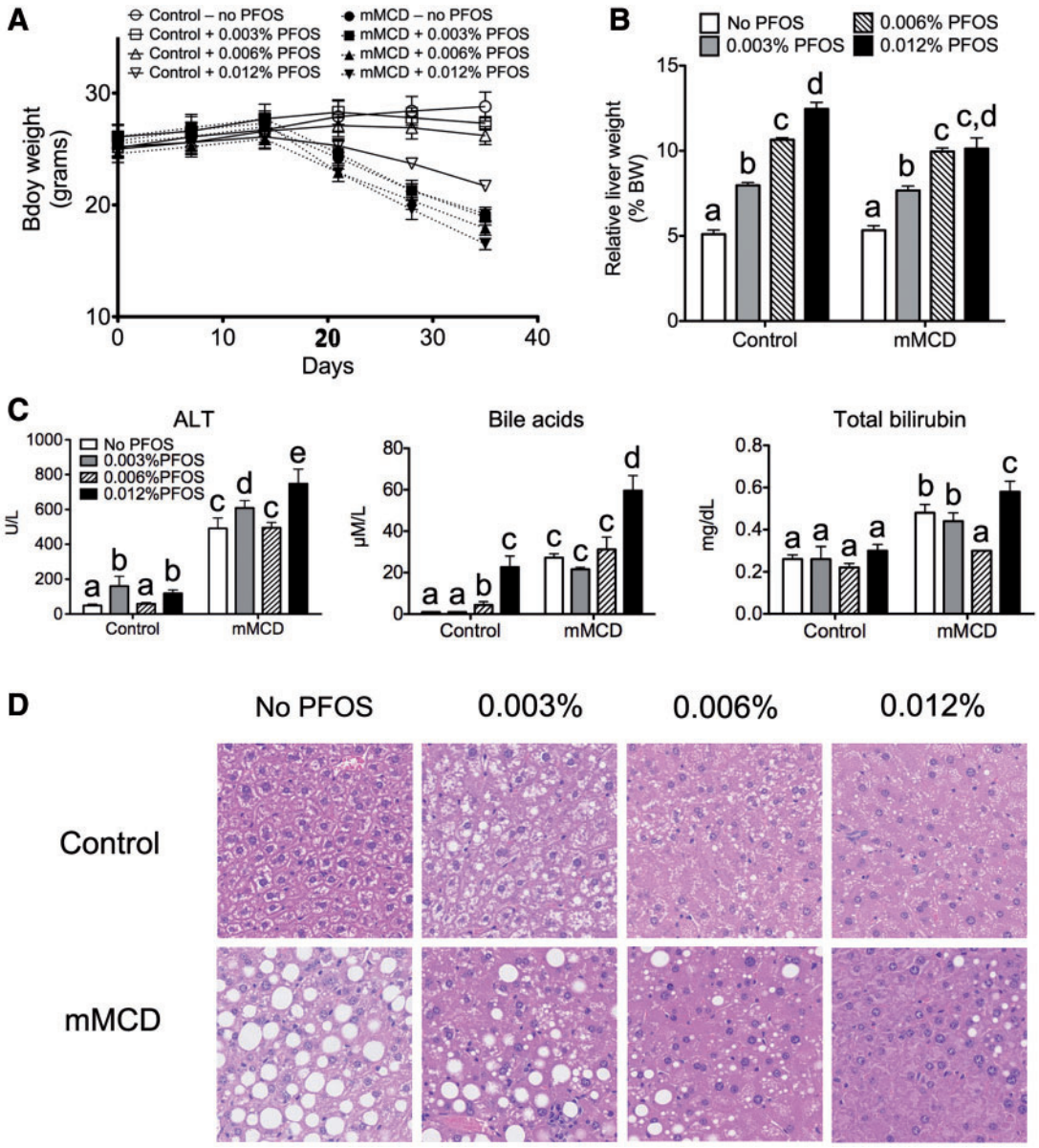

FIG. 2. mMCD exacerbates the effect of low dose PFOS exposure. A, Average weekly body weight. Mice were fed a control or mMCD diet, with or without the indicated concentration of PFOS (w/w). Treatment with dietary PFOS began after 2 weeks of acclimation to the control diet (arrow). Statistical comparisons are in Results. B, Average relative liver weight (liver weight/body weight × 100). C, Average serum concentration of ALT, bile acids and bilirubin. D, Representative H & E stained liver sections from the treatment groups fed the control or mMCD diet, with or without the indicated concentration of PFOS. Values represent the mean ± SEM. Values with different letters are statistically significant at $P \leq .05$.

(Figure 2D). The macrovesicular vacuolation was so pronounced in many liver slides that it interfered with evaluation of other cytoplasmic features of hepatocytes. Minimal to mild mixed inflammatory cell infiltration was present in the liver of a few mice fed the mMCD diet with and without K^+PFOS, with the notable exception of mice fed the mMCD diet with 0.012% K^+PFOS (data not shown). This histologic alteration was considered to be associated with the mMCD diet rather than PFOS exposure. Occasional coagulative hepatocellular necrosis was noted in mice fed either the control or MCD diet with K^+PFOS (data not shown). The hepatocellular necrosis was observed at a low incidence, and typically consisted of 1 or a few necrotic foci within the liver. Histiocytic infiltration was sometimes associated with the necrotic foci. The hepatocellular necrosis had no discernible association with the concentration of PFOS.

Dietary K^+PFOS administration was associated with an increase in the ORO staining in the liver (Figure 3A). The degree of ORO staining in the liver samples from mice fed the mMCD diet (with or without K^+PFOS) was more pronounced than observed in mice that were fed dietary K^+PFOS (Figure 3A). Interestingly, in mice fed the mMCD diet, the highest level of ORO staining was present in the low dose K^+PFOS group (0.003%) whereas the lowest level of ORO staining was present in the high dose K^+PFOS group (0.012%). The level of ORO staining in the 0.006% K^+PFOS group was intermediate, and generally equivalent to control levels (Figure 3A). In general, the observations noted for ORO staining were consistent with those found with osmium staining (data not shown).

Consistent with the ORO and osmium histological analyses, the concentration of hepatic triglycerides was increased by

dietary K^+PFOS compared with mice fed the control diet (Figure 3B). The concentration of hepatic triglycerides was higher in mice fed the control mMCD diet as compared with control mice (Figure 3B). Although not statistically significant, there was a dose-dependent downward trend in hepatic triglycerides in mice fed the mMCD diet supplemented with K^+PFOS, which was consistent with the incidence of microvesicular/macrovesicular lipid accumulation seen with H&E staining (Figure 2D) and ORO staining (Figure 3A).

The hepatic concentration of PFOS increased dose-dependently in mice fed the control and the mMCD diet at the end of the experimental feeding period (Figure 3C). However, the concentration of PFOS in the liver of mice fed the mMCD diet was lower as compared with mice fed the control diet

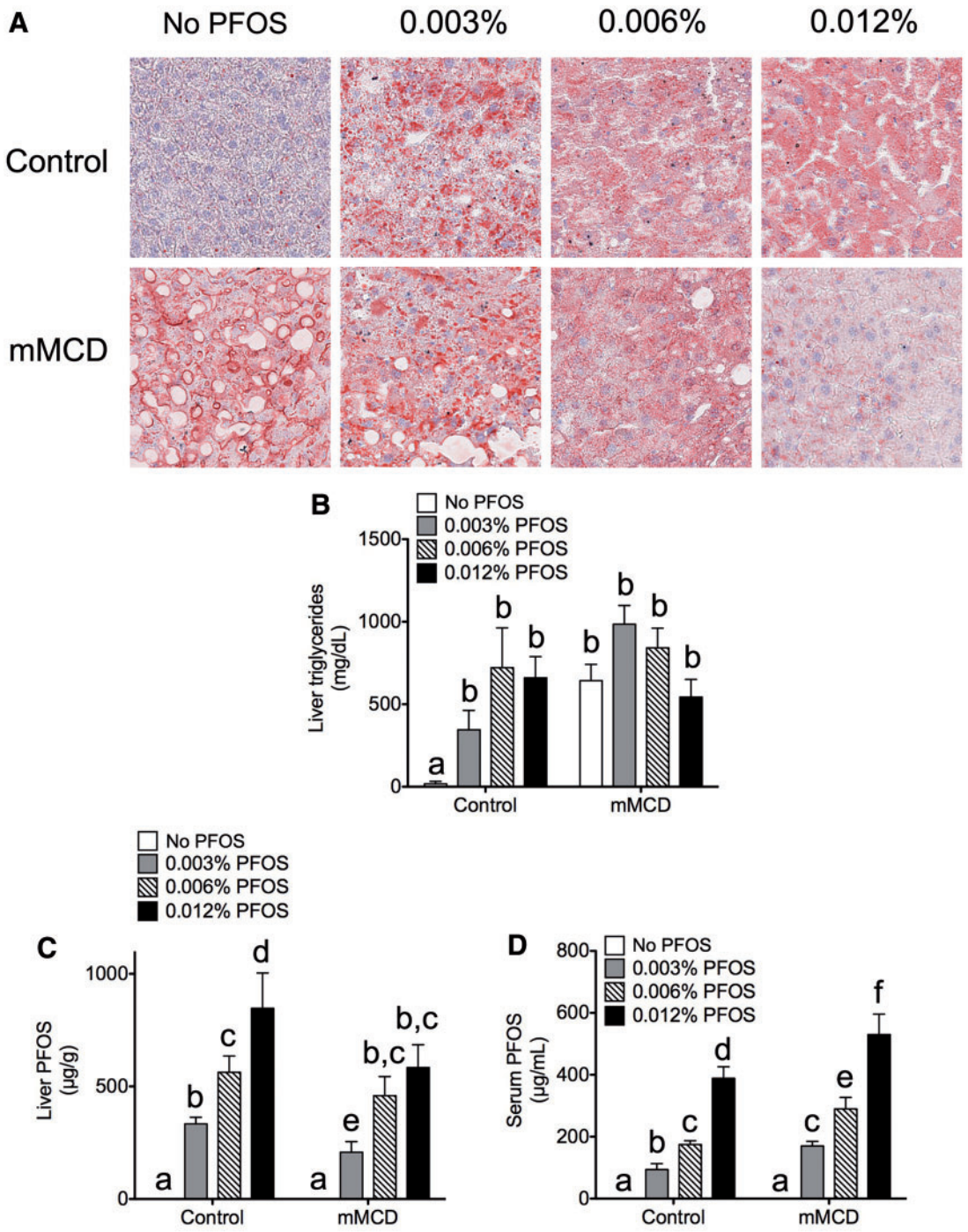

FIG. 3. Effect of an mMCD diet on PFOS-induced changes in hepatic lipids and average tissue PFOS concentration. A, Representative ORO-stained liver sections from the treatment groups fed the control or mMCD diet, with or without the indicated concentration of PFOS. B, Average hepatic concentration of triglycerides. C, Average hepatic PFOS concentration. D, Average serum PFOS concentrations. Values represent the mean ± SEM. Values with different letters are statistically significant at $P \leq .05$.

supplemented with similar concentrations of K^+PFOS (Figure 3C). There was also a dose-dependent increase in the average concentration of serum PFOS in mice fed either the control or mMCD diet (Figure 3D). Although there was a dose-dependent increase in the average concentration of serum PFOS in mice fed the control diet supplemented with K^+PFOS, the average serum concentration was lower as compared with similarly PFOS-treated mice fed the mMCD diet (Figure 3D). These differences in liver and serum PFOS concentration were not due to differences in uptake/excretion of dietary PFOS as no differences in fecal or urinary PFOS content were observed regardless of the diet type (Figure 4). Regression analyses also verified these differences in hepatic and serum PFOS concentrations between the mice fed the control and mMCD diets with K^+PFOS (Figs. 5A and B). These differences in liver and serum PFOS concentration between mice fed the control or mMCD diet supplemented with K^+PFOS were noted after one and three weeks of treatment with 0.012% dietary K^+PFOS in the liver, but only after three weeks in serum (Figs. 5C and D).

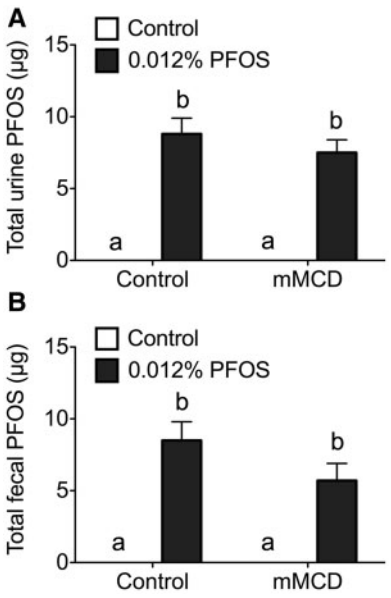

FIG. 4. Urinary and fecal PFOS after control of mMCD diet, with and without dietary (0.012%) PFOS. The concentration of PFOS was determined as described in Materials and Methods section, and the amount of PFOS determined by multiplying by the mass or volume of feces or urine, respectively. Values with different letters are statistically different at $P \leq .05$.

Supplemental Dietary Choline Prevents Hepatic Effects Induced by Low Dose Exposure to PFOS

Because the previous studies suggested that limiting dietary choline enhanced the hepatic effects of PFOS, and *in vitro* evidence demonstrated the formation of a PFOS-choline ion-pair complex, whether supplemental dietary choline could prevent effects induced by PFOS was examined. A dietary concentration of 0.003% K^+PFOS was chosen because preliminary studies indicated that supplemental dietary choline had little impact on body weight when the concentration of K^+PFOS in the diet exceeded 0.006% (data not shown). The dietary regimen was extended to 6 weeks given the milder effect of relatively low dose exposure to PFOS.

Average body weight was decreased by 0.003% dietary K^+PFOS after 5 weeks of feeding as compared with controls (Figure 6A). Supplemental dietary choline did not prevent this PFOS-induced change in average body weight (Figure 6A). Similarly, average relative liver weight was increased by 0.003% dietary PFOS after 6 weeks of feeding as compared with controls but supplemental dietary choline did not prevent this PFOS-induced hepatic effect (Figure 6B). It is of interest to note that after six weeks of feeding 0.003% dietary PFOS, the average serum concentration of ALT was increased as compared with controls, but this effect was largely prevented by supplemental dietary choline (Figure 6C). In contrast, after 6 weeks of feeding 0.003% dietary PFOS, the average serum concentration of alkaline phosphatase was increased as compared with controls, but this effect was not prevented by supplemental dietary choline (data not shown).

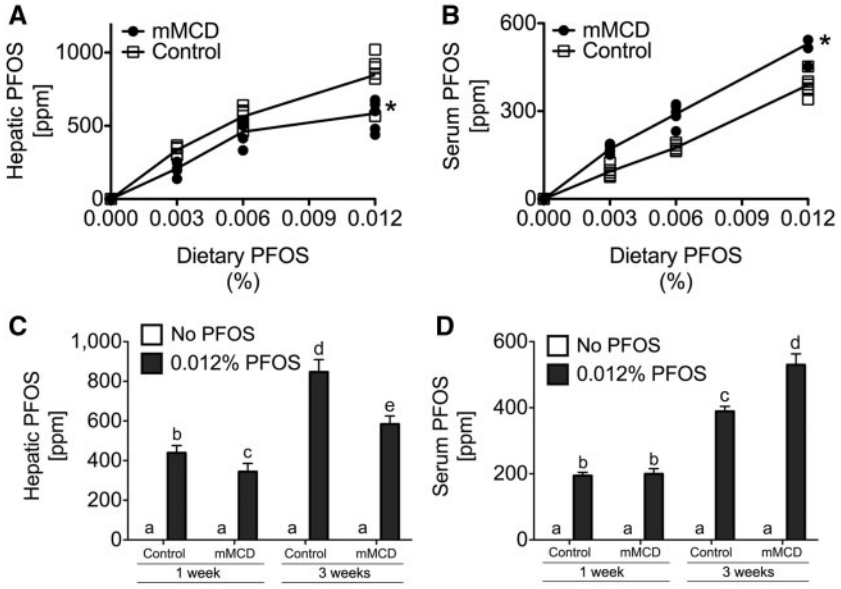

FIG. 5. Inverse correlation between liver and serum PFOS caused by mMCD diet. Regression analysis of (A) hepatic and (B) serum PFOS as compared with dietary intake of PFOS. *Significantly different than control at $P \leq .05$. (C) Hepatic and (D) serum PFOS concentration in control or mMCD fed mice after 1 or 3 weeks of diet with or without dietary PFOS (0.012%). Values represent the mean ± SEM. Values with different letters are statistically significant at $P \leq .05$.

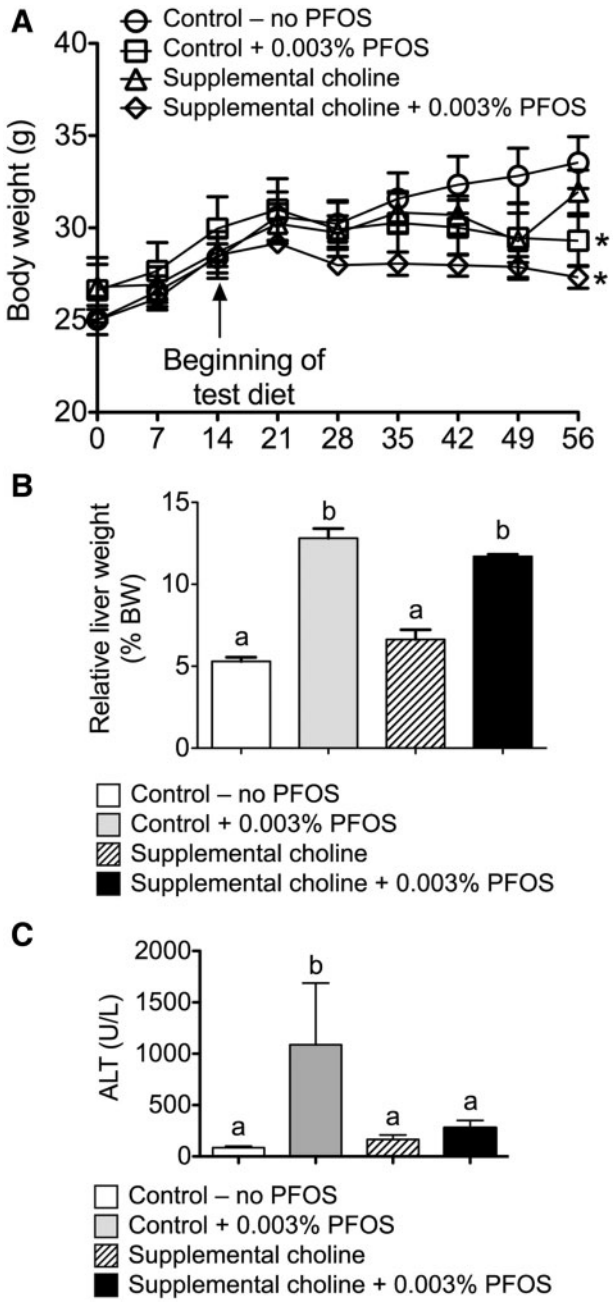

FIG. 6. Effect of supplemental dietary choline on low dose exposure to PFOS. A, Average weekly body weight. Mice were fed a control diet, control diet with supplemental choline, control diet with 0.003% PFOS, or control diet with 0.003% PFOS and supplemental choline. Treatment with dietary PFOS began after 2 weeks of acclimation to the control diet (arrow). *Significantly different than control at $P \leq .05$. B, Average relative liver weight (liver weight/body weight × 100). C, Average serum concentration of ALT. Values represent the mean ± SEM. Values with different letters are statistically significant at $P \leq .05$.

Supplemental Dietary Choline Prevents PFOS-Induced Alterations in Lipid Metabolism and Oxidative Stress

To begin to determine the mechanisms by which exposure to 0.003% K^+PFOS in the diet influences the liver, lipidomic analyses were performed. The most striking differences observed between mice fed the control diet supplemented with 0.003% K^+PFOS compared with those fed the control diet was the increase in hepatic concentrations of triglycerides, sphingomyelins and phosphatidyl cholines (Figure 7A). These data are highly consistent with the biochemical measurements and histological examinations (Figs. 2A and B). Interestingly, supplemental dietary choline reversed or prevented these hepatic changes in large part as compared with mice fed the control diet with 0.003% PFOS (Figure 7B).

One mechanism by which PFOS can potentially elicit hepatotoxicity is through increased oxidative stress. This is thought to be mediated in part by PFOS and its ability to deplete the reduced form of GSH (Liu *et al.*, 2007). Indeed, the ratio of GSH:GSSG was markedly reduced in the liver of mice fed either the control diet supplemented with 0.003% K^+PFOS or the mMCD diet as compared with mice fed the control diet (Figure 8A). Interestingly, supplemental dietary choline reversed this effect in mice fed 0.003% K^+PFOS as compared with control (Figure 8A). To determine whether this change in the ratio of GSH:GSSG was associated with oxidative stress, the concentration of hepatic MDA was measured. Mice fed the control diet supplemented with 0.003% K^+PFOS exhibited higher hepatic MDA as compared with control, and supplemental dietary choline prevented this increase in hepatic MDA (Figure 8B). Similarly, mice fed the mMCD diet exhibited an average higher hepatic concentration of MDA, and this effect was exacerbated in mice fed the mMCD diet supplemented with 0.003% K^+PFOS (Figure 8B).

DISCUSSION

In laboratory studies, liver has been shown to be the target organ with exposure to PFOS and a hallmark histological observation is hepatic lipid accumulation and oxidative stress observed in non-clinical animal models (Seacat *et al.*, 2002). Results from the present study are the first to provide evidence of a potential novel mechanism by which PFOS causes hepatic steatosis in male C57BL/6 mice (Figure 9A) and that dietary supplementation of choline may prevent and/or attenuate hepatic steatosis induced by PFOS in mice (Figure 9C).

Because PFOS is a surfactant that preferentially resides in the air/membrane surface, one plausible hypothesis that could explain these hepatic effects elicited by PFOS is its potential to interfere with the membrane function, in part, by interacting with choline, because it is one of the important precursors in the synthesis of phospholipid membrane bilayers. This hypothesis is supported by the present studies because the data demonstrated that PFOS can form a stable ion pair with choline *in vitro* (Figure 1), the observed distribution of tissue PFOS in a model with reduced dietary choline is consistent with the hypothesis that hepatic choline sequesters PFOS, and supplemental dietary choline prevented PFOS-induced oxidative stress. Alternatively, it has also been shown that PFOS may interfere with membrane function by directly influencing membrane fluidity (Xie *et al.*, 2010).

Previous studies in both rodents and humans demonstrate that dietary choline deficiency can cause hepatic steatosis (Anstee and Goldin, 2006; Buchman *et al.*, 1995). Results from this study confirmed this effect but also showed that hepatic steatosis is found in mice fed a control diet supplemented with K^+PFOS. Although the hepatic effects induced by dietary PFOS are exacerbated when mice are co-administered an mMCD diet (Figure 9B), supplemental dietary choline attenuated the oxidative stress induced by feeding a control diet with 0.003% K^+PFOS.

Dietary PFOS exposure caused a dose-dependent increase in PFOS concentrations in both liver and serum compared with

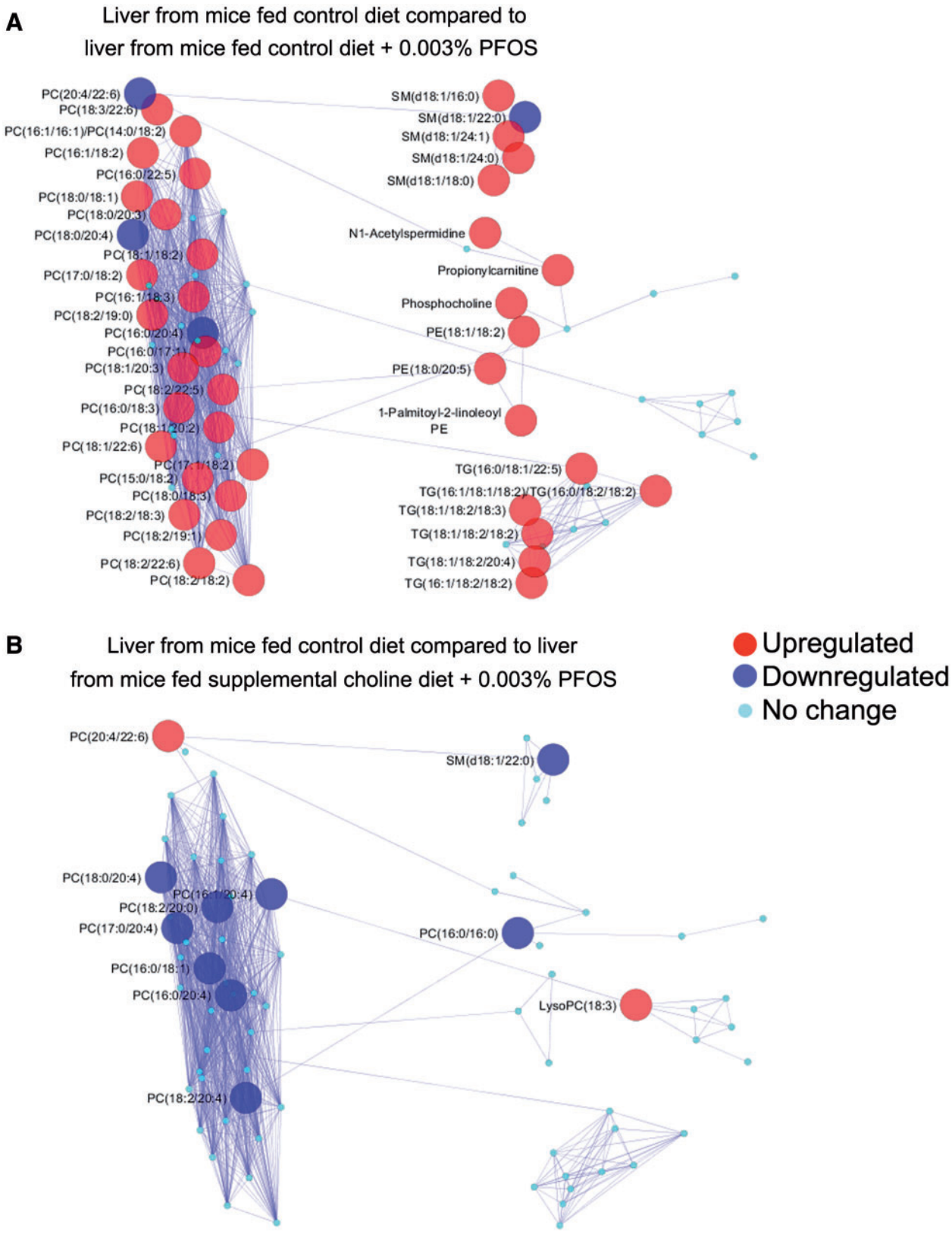

FIG. 7. Supplemental dietary choline prevents the effects of low dose PFOS exposure on hepatic lipids. A, Comparison of hepatic lipid classes in response to PFOS. Note large number of increased changes in various lipids. B, Comparison of PFOS-induced changes in hepatic lipids after supplemental dietary choline. Note large decrease in many lipids in particular triglycerides.

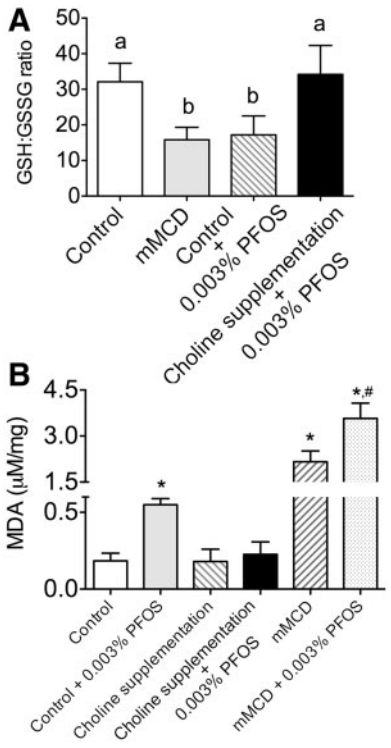

FIG. 8. Supplemental dietary choline prevents PFOS-induced hepatic oxidative stress. A, Effect of mMCD diet, PFOS and supplemental dietary choline on hepatic GSSG:GSH ratio. B, Effect of supplemental dietary choline on hepatic MDA in response to PFOS. Values represent the mean ± SEM. *Significantly different than control at $P \leq .05$. #Significantly different than mMCD control at $P \leq .05$. Values with different letters are statistically significant at $P \leq .05$.

mice fed the control diet. In contrast, it is of interest to note that serum PFOS concentrations were higher in mice fed the mMCD-based PFOS diets and liver PFOS concentrations were lower in mice that were fed PFOS incorporated in the mMCD diets. These observations support the hypothesis that PFOS causes hepatic steatosis and oxidative stress by forming an ion pair and reducing the available liver choline required for VLDL export. Efforts to measure the presence of this ion pair *in vivo* are challenging and further complicated by the fact these ion pairs form directly in the source of the mass spectrometer regardless if they exist as ion pairs or not in situ. Nevertheless, these observations are consistent with the notion that PFOS forms an ion pair with choline in the liver and reduces export of export lipids. It is possible when hepatic choline is reduced due to feeding an mMCD diet, this results in less PFOS-choline ion pair formation, causing PFOS to partition to the serum. However, further studies are needed to conclusively demonstrate the existence of an ion pair between PFOS and choline *in vivo*.

Interestingly, ORO staining was actually lower in the mice fed the mMCD diet with 0.012% K^+PFOS as compared with mice fed the control diet or the mMCD diet with lower concentrations of PFOS (0.003 or 0.006%). Although no experiments were performed to determine the mechanism(s) that underlie this effect, this observation could be due to the fact that lipid peroxides are not effectively stained by ORO as noted by others (Dixon *et al.*, 1975). Given that increased dietary PFOS can increase lipid peroxidation and oxidative stress in part due to depletion of GSH, this suggests that the relatively lower level of ORO staining observed in mice fed the mMCD diet with 0.012% K^+PFOS may reflect enhanced lipid peroxidation

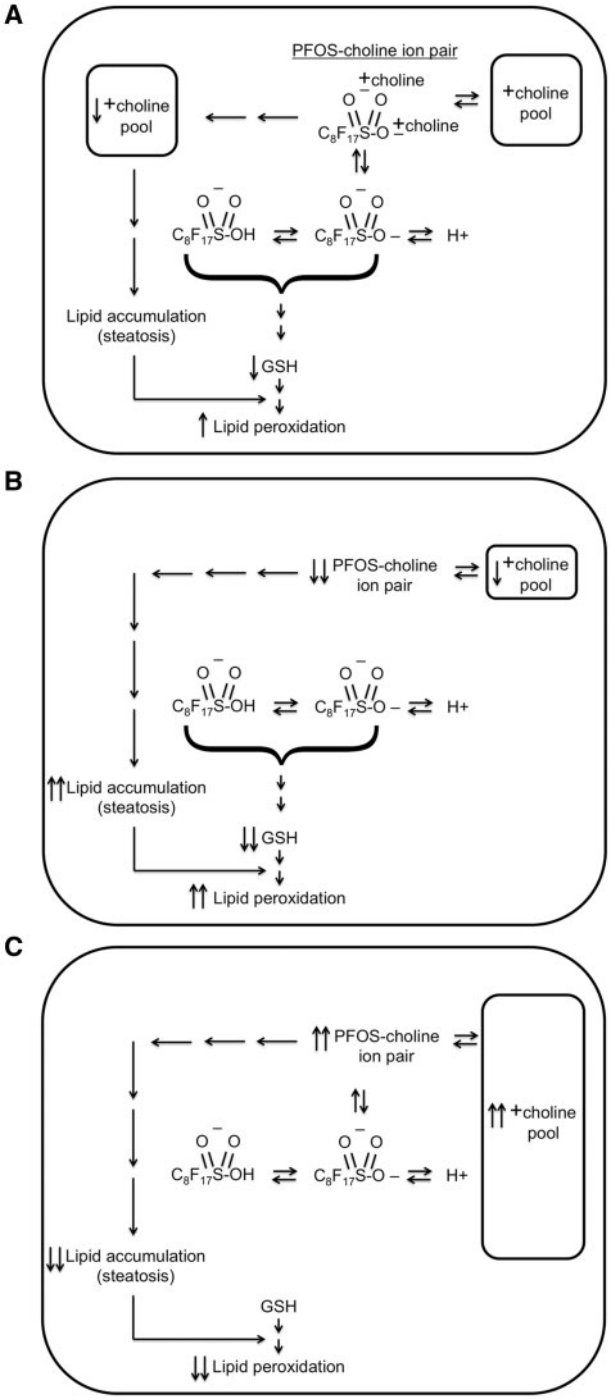

FIG. 9. Hypothetical PFOS-choline ion pair contributes to hepatic steatosis and oxidative stress. A, Under normal conditions, PFOS forms an ion pair with 2 molecules of choline, which leads to depletion of available free choline required for VLDL export. PFOS also decreases hepatic GSH. Coupled with the accumulation of hepatic lipids, the decreased GSH collectively causes an increase in oxidative stress as detected by increased lipid peroxidation and oxidative stress. B, When fed a diet with marginal dietary choline, the hypothetical PFOS-choline ion pair cannot be formed as effectively, and the reduced dietary choline causes enhanced lipid accumulation. The free PFOS causes decreased GSH, which leads to enhanced lipid peroxidation and oxidative stress. C, Supplemental dietary choline causes an increase in the hypothetical PFOS-choline ion pair. This allows for "normal" VLDL export and the lack of lipid accumulation. The amount of free PFOS available to decrease GSH is also reduced due to increased PFOS-choline ion pair formation, thus GSH levels are not decreased significantly and this prevents increased lipid peroxidation and oxidative stress.

as compared with the other mice fed lower concentrations of PFOS in the mMCD diet.

PFOS can activate the nuclear receptor PPARα (Bjork *et al.*, 2011; Elcombe *et al.*, 2012; Wolf *et al.*, 2008). Although there is some evidence that ligand activation of PPARα may be useful for preventing steatosis (Fuchs *et al.*, 2016), there are many genes that are regulated by activation of hepatic PPARα that could also contribute to steatosis (Mattijssen *et al.*, 2014). Further studies are necessary to determine whether this mechanism contributes to PFOS-induced steatosis, including whether the concentration of PFOS required to activate PPARα *in vivo* is achievable for this purpose.

Results from this study show that supplemental dietary choline can attenuate PFOS-induced effects such as impaired oxidative stress in male C57BL/6 mice. These data strongly support the hypothesis that PFOS can form an ion pair with choline in the liver and that this molecular mechanism may be suitable to target to prevent steatosis and oxidative stress in mouse liver by supplemental dietary choline (Figure 9C).

FUNDING

This work was supported by an unrestricted gift from The 3M Company.

ACKNOWLEDGEMENTS

We thank Dr George A. Parker of WIL Research for technical support with the histopathological analyses of liver samples. LC-MS/MS was performed with an instrument purchased under NSF-MRI award CBET-1126373. The authors acknowledge that John L. Butenhoff, Shu-Ching Chang, Bradley D. Bagley, and David J. Ehresman were or are employees of 3M Company, a former manufacturer of PFOS. The authors acknowledge that Dr Peters has an unrestricted gift to support research in this area, but the funding organization does not have control over the resulting publication.

REFERENCES

Akiyama, T. E., Nicol, C. J., Fievet, C., Staels, B., Ward, J. M., Auwerx, J., Lee, S. S., Gonzalez, F. J., and Peters, J. M. (2001). Peroxisome proliferator-activated receptor-α regulates lipid homeostasis, but is not associated with obesity: studies with congenic mouse lines. *J. Biol. Chem.* **276**, 39088–39093.

Anstee, Q. M., and Goldin, R. D. (2006). Mouse models in non-alcoholic fatty liver disease and steatohepatitis research. *Int. J. Exp. Pathol.* **87**, 1–16.

Bijland, S., Rensen, P. C., Pieterman, E. J., Maas, A. C., van der Hoorn, J. W., van Erk, M. J., Havekes, L. M., Willems van Dijk, K., Chang, S. C., Ehresman, D. J., *et al.*, (2011). Perfluoroalkyl sulfonates cause alkyl chain length-dependent hepatic steatosis and hypolipidemia mainly by impairing lipoprotein production in APOE*3-Leiden CETP mice. *Toxicol. Sci.* **123**, 290–303.

Bjork, J. A., Butenhoff, J. L., and Wallace, K. B. (2011). Multiplicity of nuclear receptor activation by PFOA and PFOS in primary human and rodent hepatocytes. *Toxicology* **288**, 8–17.

Buchman, A. L., Dubin, M. D., Moukarzel, A. A., Jenden, D. J., Roch, M., Rice, K. M., Gornbein, J., and Ament, M. E. (1995). Choline deficiency: a cause of hepatic steatosis during parenteral nutrition that can be reversed with intravenous choline supplementation. *Hepatology* **22**, 1399–1403.

Chang, S. C., Noker, P. E., Gorman, G. S., Gibson, S. J., Hart, J. A., Ehresman, D. J., and Butenhoff, J. L. (2012). Comparative pharmacokinetics of perfluorooctanesulfonate (PFOS) in rats, mice, and monkeys. *Reprod. Toxicol.* **33**, 428–440.

Dixon, M. F., Dixon, B., Aparicio, S. R., and Loney, D. P. (1975). Experimental paracetamol-induced hepatic necrosis: A light- and electron-microscope, and histochemical study. *J. Pathol.* **116**, 17–29.

Elcombe, C. R., Elcombe, B. M., Foster, J. R., Chang, S. C., Ehresman, D. J., and Butenhoff, J. L. (2012). Hepatocellular hypertrophy and cell proliferation in Sprague-Dawley rats from dietary exposure to potassium perfluorooctanesulfonate results from increased expression of xenosensor nuclear receptors PPARα and CAR/PXR. *Toxicology* **293**, 16–29.

Fahy, E., Sud, M., Cotter, D., and Subramaniam, S. (2007). LIPID MAPS online tools for lipid research. *Nucleic Acids Res.* **35**, W606–W612.

Folch, J., Lees, M., and Sloane Stanley, G. H. (1957). A simple method for the isolation and purification of total lipides from animal tissues. *J. Biol. Chem.* **226**, 497–509.

Fuchs, C. D., Traussnigg, S. A., and Trauner, M. (2016). Nuclear receptor modulation for the treatment of nonalcoholic fatty liver disease. *Semin. Liver Dis.* **36**, 69–86.

Hansen, K. J., Clemen, L. A., Ellefson, M. E., and Johnson, H. O. (2001). Compound-specific, quantitative characterization of organic fluorochemicals in biological matrices. *Environ. Sci. Technol.* **35**, 766–770.

Kind, T., Liu, K. H., Lee do, Y., DeFelice, B., Meissen, J. K., and Fiehn, O. (2013). LipidBlast in silico tandem mass spectrometry database for lipid identification. *Nat. Methods* **10**, 755–758.

Liu, C., Yu, K., Shi, X., Wang, J., Lam, P. K., Wu, R. S., and Zhou, B. (2007). Induction of oxidative stress and apoptosis by PFOS and PFOA in primary cultured hepatocytes of freshwater tilapia (Oreochromis niloticus). *Aquat. Toxicol.* **82**, 135–143.

Lu, W., Clasquin, M. F., Melamud, E., Amador-Noguez, D., Caudy, A. A., and Rabinowitz, J. D. (2010). Metabolomic analysis via reversed-phase ion-pairing liquid chromatography coupled to a stand alone orbitrap mass spectrometer. *Anal. Chem.* **82**, 3212–3221.

Marcolin, E., Forgiarini, L. F., Tieppo, J., Dias, A. S., Freitas, L. A., and Marroni, N. P. (2011). Methionine- and choline-deficient diet induces hepatic changes characteristic of non-alcoholic steatohepatitis. *Arq. Gastroenterol.* **48**, 72–79.

Mattijssen, F., Georgiadi, A., Andasarie, T., Szalowska, E., Zota, A., Krones-Herzig, A., Heier, C., Ratman, D., De Bosscher, K., Qi, L., *et al.* (2014). Hypoxia-inducible lipid droplet-associated (HILPDA) is a novel peroxisome proliferator-activated receptor (PPAR) target involved in hepatic triglyceride secretion. *J. Biol. Chem.* **289**, 19279–19293.

Olsen, G. W., Burris, J. M., Ehresman, D. J., Froehlich, J. W., Seacat, A. M., Butenhoff, J. L., and Zobel, L. R. (2007). Half-life of serum elimination of perfluorooctanesulfonate, perfluorohexanesulfonate, and perfluorooctanoate in retired fluorochemical production workers. *Environ. Health Perspect.* **115**, 1298–1305.

Seacat, A. M., Thomford, P. J., Hansen, K. J., Olsen, G. W., Case, M. T., and Butenhoff, J. L. (2002). Subchronic toxicity studies on perfluorooctanesulfonate potassium salt in cynomolgus monkeys. *Toxicol. Sci.* **68**, 249–264.

Shannon, P., Markiel, A., Ozier, O., Baliga, N. S., Wang, J. T., Ramage, D., Amin, N., Schwikowski, B., and Ideker, T. (2003). Cytoscape: a software environment for integrated models of biomolecular interaction networks. *Genome Res.* **13**, 2498–2504.

Wolf, C. J., Takacs, M. L., Schmid, J. E., Lau, C., and Abbott, B. D. (2008). Activation of mouse and human peroxisome proliferator-activated receptor α by perfluoroalkyl acids of different functional groups and chain lengths. *Toxicol. Sci.* **106**, 162–171.

Xie, W., Ludewig, G., Wang, K., and Lehmler, H. J. (2010). Model and cell membrane partitioning of perfluorooctanesulfonate is independent of the lipid chain length. *Colloids Surf. B. Biointerfaces*. **76**, 128–136.

Xu, L., Krenitsky, D. M., Seacat, A. M., Butenhoff, J. L., and Anders, M. W. (2004). Biotransformation of N-ethyl-N-(2-hydroxyethyl)perfluorooctanesulfonamide by rat liver microsomes, cytosol, and slices and by expressed rat and human cytochromes P450. *Chem. Res. Toxicol.* **17**, 767–775.